CT Based Semi-Automated Method for Pneumonia Severity in Mice

Ansh Johri[1*], Lewis Hsu [2]

[1]Deparment of Biomedical Engineering, Columbia University, New York, NY 10027; [2]National Institutes of Health, National Heart, Lung, Blood Institute, Washington, DC 20010.

Abstract

Misdiagnosis of community-acquired pneumonia is an important clinical problem, leading to a high rate of mortality. Diagnoses are typically conducted using two-dimensional chest x-rays, which have shown to be time-consuming and inaccurate. In an effort to improve the current diagnostic method, we utilized Micro-Computed Tomography (MicroCT) and image analysis software to develop a diagnostic algorithm that can quantitatively assess the severity of pneumonia in mice. We believed this method would provide more immediate, precise, and accurate diagnoses as opposed to the qualitative assessments done by radiologists at present, because MicroCT provides opportunities for non-invasive radiographic endpoints for pneumonia studies. A quantitative scoring of previously obtained Computed Tomography (CT) scans of pneumonia infected and control mice lungs was developed with a semi-automated image segmentation algorithm. At the endpoint of 168 hours, each of the mice was categorized as either a) a Saline (control)-injected mouse (total=13), a Pneumonia-injected Survivor (total=11), or a Pneumonia-injected Non-survivor (total=11). Three comparison tests were then completed, including Saline vs. All Pneumonia Injected Mice, Pneumonia Survivors vs. Pneumonia Non-survivors, and All Survivors (both Saline & Pneumonia) vs. Pneumonia Non-survivors. In all three comparisons, the semi-automated algorithm was better able to distinguish between the different groups than radiologists using two-dimensional chest x-rays of the mice's lungs, with p-values of 0.001, 0.039, and 0.001 for the semi-automated algorithm, and 0.004, 0.581, 0.058 for the radiologists, respectively.
Key Words: Community-acquired pneumonia, Computed Tomography

BIOMEDICAL ENGINEERING

Introduction

In the United States, pneumonia is the sixth leading cause of death and the number one infectious disease killer (M. S. Niederman, 1998). The disease is an inflammation of one or both lungs caused by an infection from bacteria, viruses or fungi. The infection causes the alveoli of the lungs to become inflamed and filled with fluid, which leads to symptoms such as cough, fever and respiratory breathing difficulties (Jelic, 2005). Often times, pneumonia occurs as a secondary infection when the immune system of a person is already weakened due to prior infection, such as an upper respiratory tract infection. This primary infection causes inflammation in the inner lining of airways that leaves the patient susceptible to the secondary infections such as pneumonia (Boone, 2004).

Pneumonia can be classified according to the population affected. Hospital-acquired pneumonia is acquired when a patient breathes germs during a hospital stay for another illness. People are most prone to hospital-acquired pneumonia while on a mechanical ventilator, since potentially pneumonia-causing bacteria and viruses may be blown directly into the lungs. The most common type of pneumonia is community-acquired. Community-acquired pneumonia is acquired outside of hospitals and other health care settings, with about 5.6 million people getting infected every year in the USA and 1.1 million requiring hospitalization (M. S. Niederman, 1998). Community-acquired pneumonia is an important clinical problem, with high rates of misdiagnosis and mortality. Current methods to diagnose pneumonia rely on two dimensional (2D) chest X-rays, which are known to have low sensitivity early in the course of pneumonia (Mohd). Radiologists typically score six lung zones (upper, middle, and lower, on the right and left sides) for each patient on a scale of 0 to 4, such that zero is normal, and the maximum possible abnormal score is 24 for the combined zones; 0 represents 0% pneumonia involvement, 1 represents up to 25% involvement, 2 represents up to 50%, 3 represents up to 75%, and 4 represents up to 100% (Armbrust, 2005). These chest X-rays may take days to diagnose the severity of pneumonia, in which time immunocompromised patients, such as patients with HIV/AIDS, cancer, diabetes, or sickle cell anemia, may reach a severity beyond curing (Smergal, 2008; Stuart, 2008). For example, immunocompromised patients with pneumonia have a mortality rate of 12% (Mohd). Furthermore, radiologists are often inconsistent with their diagnoses; two radiologists may judge the severity of pneumonia in patients very differently, leading to possible misdiagnosis (L Hsu, 2007). Thus, imaging techniques to evaluate pneumonia earlier and with more accuracy would be important diagnostic tools for clinicians. Imaging information could also be used to guide decisions on the clinical care needed, such as whether to hospitalize or to treat the patient at home, thus improving pneumonia diagnosis.

Received Dec. 31, 2009. Accepted Feb. 8, 2010. Published April 1, 2011.
*To whom correspondence should be addressed: Center for Cancer and Blood Disorders, West 4-600. Children's National Medical Center111 Michigan Ave., N.W. Washington, DC 20010
aj2381@columbia.edu

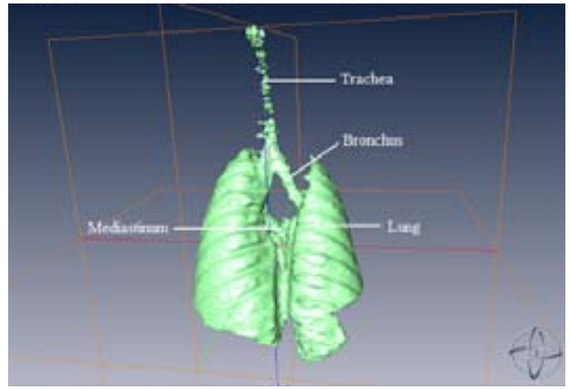

Figure 1 *3D Reconstructed Lung (Unmodified) - An image of the lung after reconstruction, containing the trachea, mediastinum, and the stomach bubble, which are subsequently removed since they cannot be infected by pneumonia.*

In order to address these limitations of inaccuracy, inconsistency, and delayed diagnosis, a different diagnostic method is required. Computed Tomography (CT) scans use X-rays that pass through the specimen and are received by sensors on the other end. Denser portions of the specimen result in a reduced amount of radiation received by the other end, since the specimen hinders the radiation. This disparity in densities, or attenuation, can be reconstructed to produce a 3D image with different grayscale values **(Figure 1)**. Hounsfield Units (HU) are grayscale values that correspond to the density of each voxel. In the Hounsfield scale, -1000 represents air, 0 represents water, and 1000 represents bone density. Notably, fluid or pus in the alveolar sacs would be approximately 0 HU, normal lung alveoli have a mixture of air and tissue reading near -500 HU, and voxels in lung with a mixture of air and fluid would be between -500 and 0 HU. CT scans, which can visualize the entire lung as opposed to the 2D projection scans in a chest radiograph, might have the sensitivity to assess the severity of pneumonia as early as 24 hours after onset. This earlier timeframe for treatment would allow immunocompromised patients to receive immediate treatment, thus decreasing their mortality rate. Since CT scans provide a more detailed depiction of the lung, they are potentially more accurate than the current chest X-ray method. Finally, by developing a semi-automated method that uses CT scans to diagnose the severity of pneumonia, more precise diagnoses can be conducted, since the procedure is more automated and less prone to human error (Muller, 2006).

The purpose of this particular research was to develop an algorithm to measure the severity of pneumonia in mice through Micro-Computer Tomography (MicroCT) Scan Analysis and test its effectiveness through comparison with radiologists' diagnosis. MicroCT works in the same way as a regular CT scanner, but is typically used to image smaller specimens, such as rodents, as opposed to human beings. There were three goals for the image analysis algorithm. The first was to achieve high reproducibility in repeated analysis of the same MicroCT scan. Current methods typically involve having two radiologists independently score the chest X-rays; the final score is then the average of the independent scores. The second goal was to achieve higher accuracy using image segmentation algorithm to quantify the amount of pneumonia in the lungs. This is different from current methods which require radiologists to qualitatively assess multiple images of pneumonia. The quantification would be done by loading the CT scans in an imaging software, and determining the voxel distribution in order to compare densities. Finally, the project aimed to increase efficiency in diagnosis. A semi-automated computer algorithm would allow more measurements to be taken in a smaller amount of time than with current methods, without special expertise in radiology. A computer would automatically calculate the severity of the pneumonia, which, under current circumstances, would be done by a radiologist. In order to use the computer algorithm method, it would be necessary for the radiologist to have some basic skills, however. The first is the ability to use Amira, the software used in this paper. The second is knowledge of basic lung anatomy, such as the location of the trachea, stomach bubble, and mediastinum. Finally, the radiologist would need the ability to use a quantitative diagnosis performed by the computer to give the correct treatment to the patient.

BIOMEDICAL ENGINEERING

We hypothesized that in vivo MicroCT scans of mice with early bacterial pneumonia could be scored quantitatively by semi-automated imaging methods, with good reproducibility and correlation with the bacterial dose inoculated, pneumonia survival outcome, and radiologists' scores previously obtained.

Materials and Methods

The project used MicroCT scans to evaluate a murine model of bacterial pneumonia through image analysis by semi-automated segmentation and comparison of results to

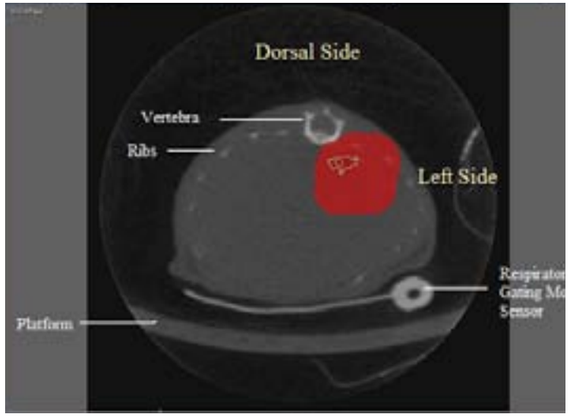

Figure 2a *Axial Lung Slice (Manual Exclusion of Stomach Bubble) - A projection view of Amira being used to eliminate the stomach bubble from the lung.*

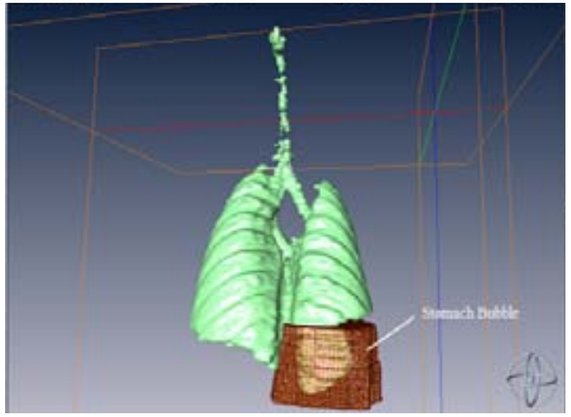

Figure 2b *3D Reconstructed Lung (Manual Exclusion of Stomach Bubble) - View of Amira selecting stomach bubble, which will then be removed from the lung.*

radiologists' interpretation. The following steps were used in the research to prepare mice with pneumonia, and then determine and validate the severity of their pneumonia:

1. Inoculation of mice with different severities of pneumonia bacteria and acquisition of CT scans (L Hsu, 2007)

2. Radiologists' diagnosis of pneumonia (L Hsu, 2007)

3. Pneumonia diagnosis using semi-automated diagnostic algorithm

The first two steps were done prior to this project, whereas the third step was conducted specifically in this research, and performed by one individual, with three trials for each mouse. Mercury Computer Systems' Amira 4.1 software was used to perform image analysis of the CT scans. Amira can perform image segmentation, 3D visualization, and other image processing (Schimel, 2007). Since the severity of pneumonia can be assessed by the volume distribution of materials within the lung due to inflammation, it was expected that more lung volume distribution in the range of high attenuation for greater severities of pneumonia would be observed (L Hsu, 2007). After loading the stack of typically near 400 axial slices for 3D reconstruction in Amira, the lung was reconstructed by selecting Hounsfield units -510 to 0 (Muller, 2006). Non-lung anatomical structures overlapping or in the vicinity of the lungs in the mice CT scans were excluded from the lung reconstruction because these structures are not involved with pneumonia infection **(Figures 2a, 2b, and 3)** (Iwaki, 2001). The non-lung components that overlapped with the lungs were primarily the stomach bubble, trachea, and mediastinum (Armbrust, 2005). The algorithm excluded each of these components systematically using the image manipulation features of Amira. All subsequent non-3D images were axial cross-sections of the upper mouse body. The stomach bubble is a pocket of air that lies right below the lung. The contents in this bubble fall in the Hounsfield Unit range of -510 to 0 and also border the lung. Therefore, when a region in the lung within this range was clicked, the stomach bubble was included in the selection as well. The stomach bubble was manually removed, as shown in Figures 2a and 2b. Like the stomach bubble, the trachea is attached to the lung and gets selected in the -510 to 0 range. To remove it, the trachea was cut off at the carina, the point at which the two bronchi join to become the trachea. The same procedure used in the stomach bubble removal was then used for trachea removal **(Figure 3)**. The mediastinum is the anatomic region comprising a group of structures between the lungs that includes blood vessels and the esophagus. It was at times hard to distinguish between lung and mediastinum, making separation of mediastinum difficult in many scans. However, since the mediastinum accounts for such a small percentage of the lung volume, its effect on the voxel quantification was negligible, essentially eliminating human error. The procedures for removing of stomach bubble and trachea were used to remove the mediastinum as well. At this point, the trachea, stomach bubble, and mediastinum had been removed from the lungs. Therefore, the image reconstructed contained only those voxels that could be affected by pneumonia. This image was now ready for segmentation **(Figure 4)**.

The lung was segmented into eight regions using the following steps. The density ranges of each of the eight materials, named Well-Aerated Lung, B, C, D, E, F, G, and H were created, with Hounsfield values of -510 to -350, -350 to -300, -300 to -250, -250 to -200, -200 to -150, -150 to -100, -100 to -50, and -50 to 0, respectively. These materials were entered into the "Label Voxel" tool, generating these 8 distinct density ranges within the entire CT scan. Figure 5 illustrates this procedure: The materials "Well-Aerated Lung," "B," and "C," encapsulate all voxels inside the entire scan within the density ranges of -510 to -350, -350 to -300 and -300 to -250, respectively **(Figure 5)**. The tool can only analyze three materials at a time, but this had a negligible effect on the time it took to do the quantification analysis because the analysis is almost instantaneous..

We were only interested in the volume of each material within the lung, not the entire scan, which includes bone, muscle, fat, fur, and other tissues. It should be noted that the units of the volume measurements are irrelevant, since we eventually determined the percentage distribution of each material within the lung. Using Amira, we were able to measure how much of each of the eight materials was present in the lung volume. In Table 1, the volume of each of the first three materials can be seen: outside the lung (Exterior), inside the lung (Lung), and in the whole scan (Total) **(Table 1)**.

Essentially, the semi-automated method was broken down into the three following steps. The first was the isolation of the lung from the rest of the CT scan. The second was the removal of extraneous anatomical features, such as the stomach bubble, trachea, and mediastinum, which cannot get affected by pneumonia and would therefore skew our calculations. The final step involved finding the percentage of each of the lung materials (Well-Aerated, B, C…). The voxel distribution was analyzed for each of the survival groups.

Results

In the animal facility, 24 mice inoculated with bacteria developed symptoms of pneumonia, 11 of which died by the endpoint of 168 hours. The 11 mice inoculated with saline had few or no signs of pneumonia, and none died. No mice died during the actual MicroCT scan. After monitoring the mice for 7 days, each of these 35 mice was assigned to one of three experimental groups based on survival outcome and inoculation: (1) Pneumonia Survivor (total = 13), (2) Pneumonia Non-Survivor (total = 11), and (3) Saline-Inoculated Control (total = 11).

In the development of a semi-automated method, three trials were conducted for each of the 35 mice, and the coefficient of variation (CV) was calculated to evaluate reproducibility. The semi-automated segmentation was reproducible, with the trials for each MicroCT scan resulting in the same segmentation volumes within a coefficient of variation of 2%. Although all three trials were done by the same researcher, it is doubtful that there was much bias. The procedure to do the quantification is very structured and standard. If another researcher performed the experiment, assuming that the researcher followed the exact same procedure, there should be a negligible amount of variation, since all the quantifications are automatically done by the computer, and are therefore human-independent. Grouping the MicroCT segmentation results showed the expected findings for the three experimental groups **(Table 2)**.
In the lower ranges of attenuation, Saline-Inoculated mice had the greatest percentage of lung

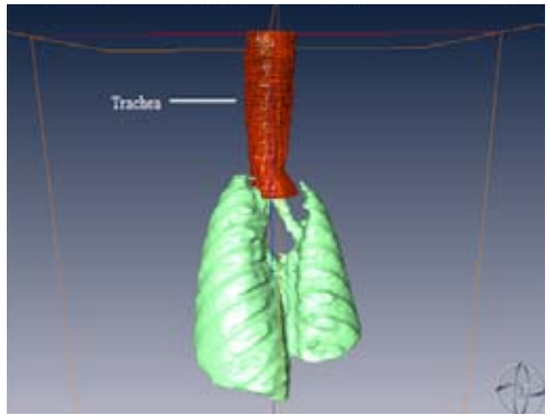

Figure 3 *3D Reconstructed Lung (Manual Exclusion of Trachea) - A 3D view of Amira selecting the trachea, which will then be removed from the lung.*

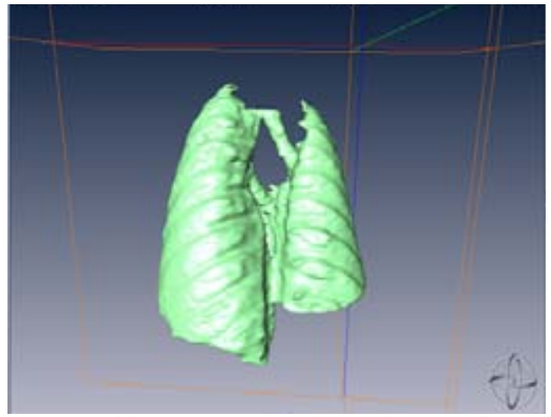

Figure 4 *3D Reconstructed Lung (Manual Exclusion of Trachea) - A 3D view of Amira selecting the trachea, which will then be removed from the lung.*

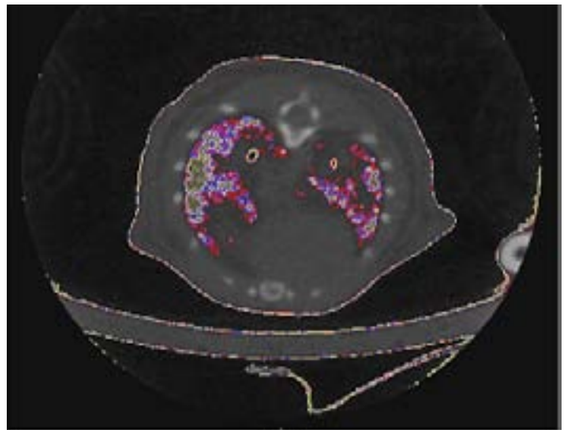

Figure 5 *Materials "Well-Aerated Lung," "B," and "C" - The beginning of the segmentation process. The three densities with lowest attenuation - Well-Aerated, B, and C - are shown in an axial view of the lung. Note that these materials lie outside of the lung, and must be disregarded from the quantification.*

volume, followed by Pneumonia Survivors, then Pneumonia Non-survivors. For example, the material with the lowest attenuation, "Well-Aerated Lung" (Hounsfield units -510 to -350), on average, made up 18.3% of lung volume in the Saline-Inoculated group, 10.9% of Pneumonia Survivors, and 8.2% of Pneumonia Non-survivors. On the other side of the density spectrum, the mice that eventually died of pneumonia had the highest percentages of lung volume in the higher ranges of attenuation, followed by Pneumonia Survivors, and finally the Saline-Inoculated group.

Table 2 presents the p-value distribution from a t-test¬ for each of the eight density ranges, for the following three experimental group comparisons: (1) Saline-Inoculated vs. All Pneumonia Infected, (2) Pneumonia Survivors vs. Pneumonia Non-Survivors, and (3) All Survivors vs. Pneumonia Non-Survivors.
Comparisons (1) and (3) were significantly different (p-value < 0.05) for all the materials except for material D (Table 2, highlighted yellow). This may indicate the density range of material D (-250 to -200) includes regions of the lung that are not affected by pneumonia, since the three experimental groups did not show significant difference in their average percentages for this material. Excluding material D, the Pneumonia Survivors vs. Pneumonia Non-Survivors comparison, however, showed no statistical significance except in material H **(Table 3, highlighted orange)**. Material H, as can be seen by Table 4, showed far greater significance by the semi-automated method than by the radiologists' scores, thus indicating that the semi-automated method was indeed more reproducible than the radiologists' method **(Table 4)**. All the materials showed more significance than the radiologists' interpretations; however, only H had a p-value under 0.05 for all three group comparisons.

A qualitative assessment of the scans was also made. Figures 6-8 show frontal pictures of three mice, each from the saline, pneumonia survivors, and pneumonia non-survivors groups, respectively **(Figures 6, 7, 8)**. The red color represents voxels in the highest third density range of the lung, the orange color represents voxels in the middle third density range, and the blue color represents the voxels in the lower third of the density range. As it can be seen, the saline mouse had the greatest amount of orange and least amount of red, the pneumonia survivor group had less orange and more red, and finally, the pneumonia non-survivor group had the least orange and most red.

Discussion

Preliminary statistical analysis of the semi-automated segmentation of MicroCT detected differences between the groups of pneumonia survivors versus pneumonia deaths. There was good reproducibility of the semi-automated segmentation, with less than 2% variability with repeated application of the methods. Radiologists' average scores provided statistically significant differences between the mice inoculated with pneumonia vs. the mice inoculated with saline, but not between the groups of pneumonia survivors vs. pneumonia non-survivors, nor between all surviving mice vs. pneumonia deaths. This comparison suggests

Table 1 ***Volume of Interest calculated by Amira software*** *- The percentages that each of the three groups had for the 8 density ranges. The pneumonia non-survivors had the greatest percent distribution in the higher lung density ranges, indicating a pneumonia-affected lung. The saline mice, however, had a greater percentage towards the lower density ranges, the opposite of the pneumonia non-survivors.*

Volume of Interest	Well-Aerated Lung	B	C
Exterior	720.2	174.7	165.4
Lung	60.20	61.95	75.21
Total	780.4	236.7	240.6

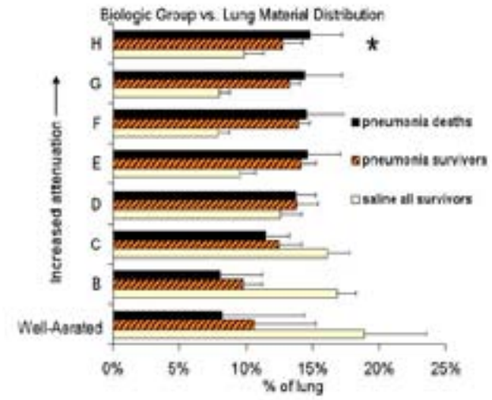

Table 2 *Average Lung Distribution for Each Group - Volumes of 3 materials, out of the total 8: a) outside the lungs (Exterior), b) inside the lungs (Lung), and c) in the entire scan (Total).*

that the semi-automated segmentation may provide a better method for quantitative scoring of pneumonia severity by CT scans, compared to scoring by radiologists.

Only a few other studies have applied quantitative image analysis to CT scans of pneumonia in animal models (M Amigoni, 2008). For example, one examined another type of bacterial pneumonia and used different methods to score the pneumonia. Another examined acid-aspiration pneumonia to score the lung injury. Their studies did not examine severity in terms of survival, and did not compare the image analysis to scoring by radiologists.

Previous applications of quantitative image analysis of lung CT scans have focused on different clinical problems, rarely pneumonia: (1) emphysema, in which lungs have abnormal pockets of low attenuation, (2) lung tumors, which have much higher attenuation than normal lungs, and (3) normal and abnormal physiologic distribution of aeration and blood flow, often using tracer materials to detect flow (Ritman, 2008). Tracers to detect blood flow include xenon, intravenous iodinated contrast, and microspheres, but since such tracers were not used in this project, the problem of distinguishing normal lung vs. high-attenuation pneumonia involvement was more difficult.

Clinical use of CT imaging is widespread throughout the world because of the wealth of information that CT scans provide about abnormal fluid, tumors, aeration, etc. Clinical High Resolution CT (HRCT) is now starting to be used to diagnose pneumonia in patients, but is rarely used for community-acquired pneumonia, which affects more people than any other type of pneumonia (Jelic, 2005). Although the spatial resolution of MicroCT is better than clinical HRCT on an absolute scale (60 microns vs. 500-1000 microns), the spatial detail is better with HRCT when considering the anatomic size of mouse lungs vs. human lungs (apex to diaphragm ~3cm vs. ~50cm, alveoli 80 microns vs. 210 microns, respectively). Thus, it can be concluded that transferring the technique

Table 3 *P-value Distribution for each Material, as calculated by t-test Comparison - Statistically significant ability for material H to distinguish between Saline vs. All Pneumonia, Pneumonia Survivors vs. Pneumonia Non-Survivors, and All Suvivors vs. Pneumonia Non-Suvivors. Radiologists were not as successful in distinguishing these groups. Material D was useless in distinguishing any of the groups apart. *Material H was significantly different for the three groups, p <.05*

Comparison	Well-Aerated Lung (-510: -350)	B (-350: -300)	C (-300: -250)	D (-250: -200)	E (-200: -150)	F (-150: -100)	G (-100: -50)	H * (-50: 0)	P-value from t-test of radiologists scores
1) Saline vs. All Pneumonia Infected	0.018	0.000	0.000	0.065	0.000	0.000	0.000	0.001	0.004
2) Pneumonia Survivors vs. Pneumonia Non-Survivors	0.375	0.298	0.317	0.946	0.672	0.622	0.296	0.039	0.581
3) All Survivors vs. Pneumonia Non-Survivors	0.032	0.007	0.010	0.448	0.043	0.031	0.009	0.001	0.058

Comparison Groups	P-value from t-test of percent lung by Semi-Automated Segmentation in material H	P-value from t-test of Radiologists scores
Saline vs. Bacteria	0.001	0.004
Pneumonia Survivors vs. Pneumonia Deaths	0.039	0.581
All Survivor vs. Bacterial Deaths	0.001	0.058

Table 4 *Comparison of MicroCT quantification by Material H to qualification by radiologists - A comparison of the ability of the semi-automated method to tell groups apart versus radiologist ability. Scoring by the semi-automated method is far more precise than the scoring by the radiologists.*

from mouse to humans should make the algorithm more accurate due to increased relative resolution. The current HRCT technique, though an improvement to the more common 2D chest X-ray method, may still provide insufficient detail for quantitative analysis of a 3-dimensional reconstruction because it generally captures only a few 2D slices (Uchiyama, 2003). Newer techniques of human spiral CT will capture enough information for the 3D reconstruction as used in our algorithm.

The principal limitation of this method was the accuracy of manually isolating the lung "volume of interest" from the rest of the mouse. It was sometimes difficult to separate the lung from nearby structures, such as the mediastinum. In the future, iodinated or other contrast materials may help more finely define these anatomical structures, until the algorithm is applied to HRCT, which provides finer resolution and, therefore, clearer anatomical structure contrast. This way, it would be easier to isolate the lung during the steps using Amira. However, the extraneous materials have a relatively small percentage in the original lung constructed, so there is still a little room for error in terms of having a slightly poor exclusion of these anatomical features. It was found that on average, even if quantifications were done having all three principal anatomical features still in the volume of interest, there would be a coefficient of variation of less than 3%, which is still well under the statistically significant threshold of 5%.The removal of the anatomical features is for lung infection consistency and improved precision.

Another limitation of this animal study was the small sample size; we intend to extend this technique to another group of mice with pneumonia. Finally, these studies examined only one strain of bacteria and

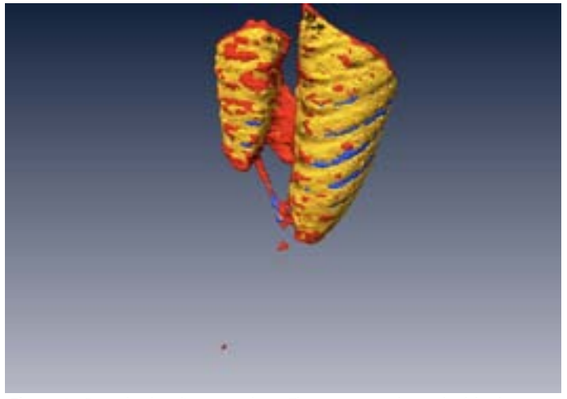

Figure 6 *Example of a saline mouse lung - The percentages that each of the three groups had for the 8 density ranges. As it can be seen, the pneumonia non-survivors had the greatest percent distribution in the higher lung density ranges, indicating a pneumonia-affected lung. The saline mice, however, had a greater percentage towards the lower density ranges, the opposite of the pneumonia non-survivors.*

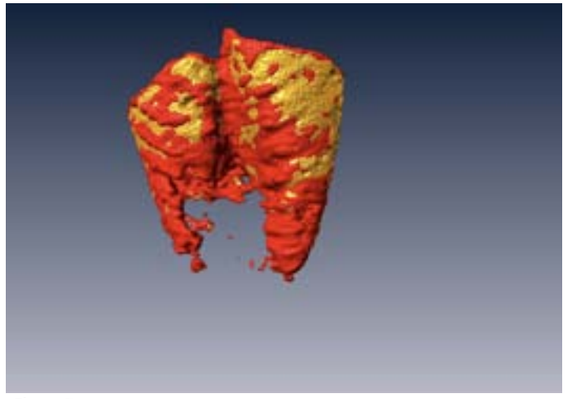

Figure 7 *Example of a pneumonia-survivor mouse lung - Frontal view of a pneumonia survivor mouse's lung. The lung has far more red shade than the saline mouse, indicating its relative high density.*

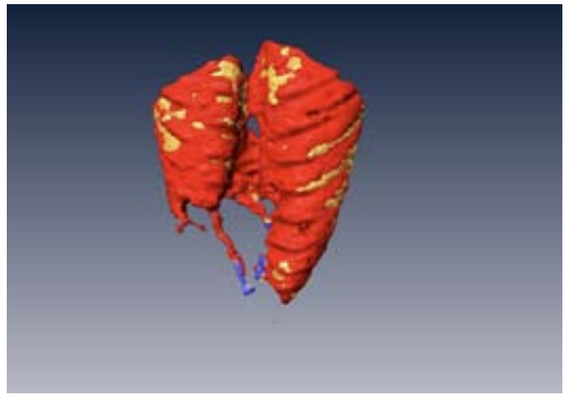

Figure 8 *Example of a pneumonia non-survivor lung - Frontal view of a pneumonia non-survivor mouse's lung. The lung is almost completely shaded red, showing that the mouse has a severely pneumonia-affected lung.*

mice, with the inclusion of antibiotics and supportive care. Extending these techniques to other mice will require additional validation, but may help to provide a non-invasive endpoint for studies with experimental pneumonia in transgenic animals. This method of quantitative assessment of pneumonia severity by CT has potential for application in clinical trials in community-acquired pneumonia, as well as other lung diseases.

References

Armbrust, LJ, Derek A. Mosier (2005). Correlation of results of pulmonary computed tomography and pathologic findings in mice with Pasteurella-induced pneumonia. American Journal of Veterinary Research 66 835-838.

Boone (2004). Small-animal X-ray dose from micro-CT. Moecular Imaging 3 149-158.

Iwaki, T (2001). A Color Atlas of Sectional Anatomy of the Mouse).

Jelic, S (2005). Pneumonia Explained - What is Pneumonia? How is Pneumonia Contracted. The New York Times Company.

L Hsu, ES, R Summers, D Koziol (2007). Computed Tomography Scans To Assess Severity of Bacterial Pneumonia in a Mouse Model.

M Amigoni, GB, S. Masson (2008). Lung injury and recovery in a murine model of unilateral acid aspiration: functional, biochemical, and morphologic characterization. Anesthesiology 108 1037-1046.

M. S. Niederman, JJM, A N Unger, A Kumar (1998). The cost of treating community-acquired pneumonia. Clin Ther.

Mohd, N A Discrimination Method for the Detection of Pneumonia Using Chest Radiograph. Computerized Medical Imaging and Graphics 160-166.

Muller, NL (2006). Pulmonary Infection: Basic Concepts. Imaging of Pulmonary Infections 1-17.

Ritman, EL (2008). Micro-Computed Tomography of the Lungs and Pulmonary-Vascular System. Proceedings of the American Thoracic Society 2 477-480.

Schimel, D (2007). Steps for Amira Procedure for Segmentation to Quantify and Visualize Lung Volume in Well-Aerated Lung and Bacterial Pneumonia.

Uchiyama, Y (2003). Quantitative computerized analysis of diffuse lung disease in high-resolution computed tomography. Medical Physics 30.